Journal of Power Sources 245 (2014) 89–94

Contents lists available at SciVerse ScienceDirect

Journal of Power Sources

journal homepage: www.elsevier.com/locate/jpowsour

Nickel and cobalt electrodeposited on carbon fiber cloth as the anode of direct hydrogen peroxide fuel cell

Fan Yang, Kui Cheng, Xue Xiao, Jinling Yin, Guiling Wang, Dianxue Cao*

Key Laboratory of Superlight Material and Surface Technology of Ministry of Education, College of Material Science and Chemical Engineering, Harbin Engineering University, Harbin 150001, China

HIGHLIGHTS

- Ni and Co supported on carbon fiber cloth is prepared by electrodeposition.
- High performance direct peroxide–peroxide fuel cells (DPPFC) are demonstrated.
- The DPPFC displays a peak power density of 21.6 mW cm^{-2} at 20 °C.

ARTICLE INFO

Article history:
Received 21 April 2013
Received in revised form
19 June 2013
Accepted 19 June 2013
Available online 28 June 2013

Keywords:
Nickel
Cobalt
Electrodeposition
Hydrogen peroxide
Electrooxidation
Fuel cell

ABSTRACT

Carbon fiber cloth (CFC) supported Ni and Co electrodes are prepared by electrodeposition (Ni/CFC and Co/CFC). Their catalytic performance for H_2O_2 electrooxidation in KOH solution is investigated and compared with Au/CFC electrode. Ni/CFC electrode exhibits higher catalytic activity than Au/CFC and Co/CFC electrodes. The performance of a direct peroxide–peroxide fuel cell (DPPFC) with Ni/CFC anode and Pd/CFC cathode is examined. The cell shows a peak power density of 21.6 mW cm^{-2} at 20 °C and 53.8 mW cm^{-2} at 50 °C. The cell performance is improved with the increase of anolyte and catholyte flow rate and operation temperature. Results indicates that the performance of DPPFC with low-cost Ni/CFC anodes is comparable with those using precious metal anodes, e.g., Au/CFC and Pd/CFC.

1. Introduction

Hydrogen peroxide (H_2O_2) has been exploited as a carbon-free energy carrier that can be used as both fuel and oxidant in a fuel cell, namely direct peroxide–peroxide fuel cell (DPPFC) [1–10]. Recent study [6] has reported that H_2O_2 can be produced using electrical power of a photovoltaic solar cell at nearly 100% current efficiency. The produced H_2O_2 can power a DPPFC to generate electricity, thus realizing a clean and efficient way of power generation from solar energy. DPPFC is all liquid feed fuel cell operating without air. It generates power and provides O_2 at the same time. So it is a good candidate for underwater or space power sources. As the fuel of a fuel cell, H_2O_2 is carbon-free and has none of the environmental problems associated with other fuel cells such as methanol, formic acid and hydrazine [11–14]. As the oxidant of a fuel cell, H_2O_2 has faster electroreduction kinetics than O_2 [15–19].

DPPFC can be operated in one-compartment or two-compartment configuration. Yamazaki et al. [2] first reported a membraneless one-compartment DPPFC with low open circuit voltage (OCV) and low power density. Recently, Mousavi Shaegh et al. [7] significantly improved the OCV of one-compartment DPPFC to 0.6 V and the power density to 1.55 mW cm^{-2} using Ni anode and Prussian blue cathode in an acidic medium. The two-compartment DPPFC was first established by Hasegawa et al. [20]. They demonstrated that the OCV and output power density of two-compartment DPPFC is remarkably higher than that of one-compartment configuration. We [8–10] recently reported a high performance two-compartment DPPFC using carbon fiber cloth supported noble metal (Pd, Au and Pd–Au) with special structure as both the anode and cathode. The DPPFC exhibits a stable OCV of 0.9 V and a peak power density of 20.7 mW cm^{-2} at 20 °C. We [8] also found that the cathode reaction has a much larger

* Corresponding author. Tel./fax: +86 451 82589036.
E-mail address: caodianxue@hrbeu.edu.cn (D. Cao).

0378-7753/$ – see front matter © 2013 Elsevier B.V. All rights reserved.
http://dx.doi.org/10.1016/j.jpowsour.2013.06.115

overpotential than the anode reaction, that is, H_2O_2 electrooxidation has a faster reaction kinetics than H_2O_2 electroreduction. Therefore, non-noble metals can be used as the anode catalyst to reduce the cost of DPPFC. In this investigation, we reported two non-noble metal electrodes: carbon fiber cloth (CFC) supported Ni and Co (Ni/CFC, Co/CFC). We demonstrated that the performance of DPPFC with these non-noble metal anodes is comparable with those using noble metal anodes, e.g. Au/CFC and Pd/CFC.

2. Experimental

2.1. Reagents

$PdCl_2$ (>99.9%), $HAuCl_4$ (>99.9%), $HClO_4$, $NiCl_2$, $CoCl_2$, HBO_3, KOH, H_2SO_4 and H_2O_2 were obtained from Enterprise Group Chemicals Reagent Co. Ltd. China. Carbon fiber cloth (thickness: 0.34 mm) was purchased from Shanghai Hesen electric Co., Ltd. All chemicals are analytical grade and were used as-received without further purification. Ultrapure water (Millipore, 18 MΩ cm) was used throughout the study.

2.2. Preparation and characterization of the Ni/CFC and Co/CFC electrodes

The Ni/CFC and Co/CFC electrodes were prepared by electrodeposition of metals on carbon fiber cloth, which acts as the support of metal catalysts and the current collector of the electrode. The electrodeposition was performed by a square-wave cathodic current method in a typical three-electrode electrochemical cell controlled by computerized potentiostat (Autolab PGSTAT302, Eco Chemie). The CFC (10 mm × 10 mm × 0.34 mm) served as the working electrode, which was placed between two parallel platinum foil (10 mm × 10 mm) counter electrodes. An Ag/AgCl (3 mol L^{-1} KCl) electrode was used as the reference electrode, and all potentials in this work were referred to this reference electrode. Ni deposition was carried out in 0.1 mol L^{-1} $NiCl_2$ + 0.5 mol L^{-1} HBO_3 solution under an upper limit current of −3 mA cm^{-2} and a lower limit current of −30 mA cm^{-2} with a pulse interval of 50 s and a total cycles of 20. The Co deposition was performed in 0.1 mol L^{-1} $CoCl_2$ + 0.5 mol L^{-1} HBO_3 solution under the identical deposition parameters as the Ni deposition. The Au/CFC and Pd/CFC electrodes were also prepared for comparison using our previous reported method [8,10]. Briefly, the Au/CFC electrode was prepared using square-wave potential electrodeposition in 1.0 mmol L^{-1} $HAuCl_4$ + 0.5 mol L^{-1} H_2SO_4 solution by applying 12,000 cycles of potential pulse between 1.1 V for 50 ms and −0.5 V for 50 ms. The Pd/CFC electrode was also prepared using the square-wave potential electrodeposition in 5.0 mmol L^{-1} $PdCl_2$ + 0.1 mol L^{-1} $HClO_4$ solution by applying 120,000 cycles of potential pulse between 0.5 V for 5 ms and −0.1 V for 5 ms.

The electrode morphology was characterized by a scanning electron microscope (SEM, JEOL JSM-6480). The structure was analyzed using an X-ray diffractometer (Rigaku TTR III) with Cu Kα radiation (λ = 0.1514178 nm). The Pd loading and Au loading were measured using an inductive coupled plasma emission spectrometer (ICP, Xseries II, Thermo Scientific). Dendritic Pd and Au electrodeposited on the 1.0 cm^2 CFC substrate were first dissolved in aqua regia solution and then diluted to 1.0 L solution for the ICP measurement.

2.3. Electrochemical measurements and DPPFC tests

H_2O_2 electrooxidation was performed in a three-electrode electrochemical cell with the same configuration as that for electrodeposition, except that the two Pt foil counter electrodes were placed behind D-porosity glass frits to eliminate the effect of H_2O_2 decomposition at the counter electrode on the catalytic performance. The electrolyte for H_2O_2 electrooxidation was H_2O_2-containing KOH. The reported current densities were calculated using the geometrical area of the electrode. All solutions were made with analytical grade chemical reagents and ultra-pure water (Milli-Q 18 MΩ cm). All measurements were performed at ambient temperature (20 ± 2 °C) under N_2 atmosphere.

DPPFC with the configuration shown in Fig. 1 was fabricated using the Pd/CFC electrode as the cathode and the Ni/CFC, Co/CFC and Au/CFC electrodes as the anodes, respectively. The preparation methods of membrane electrode assembly (MEA) and the fuel cell assembling were described in our previous report [9]. Nafion-115 (DuPont, USA) membrane was used to separate the anode and cathode compartments. The Pd loading in the Pd/CFC cathode is 0.3061 mg cm^{-2} and the Au loading in the Au/CFC anode is 0.1131 mg cm^{-2} (the data obtained from ICP analysis [8,10]). The discharge performance of the DPPFC was measured using a computer-controlled E-load system (Arbin, USA).

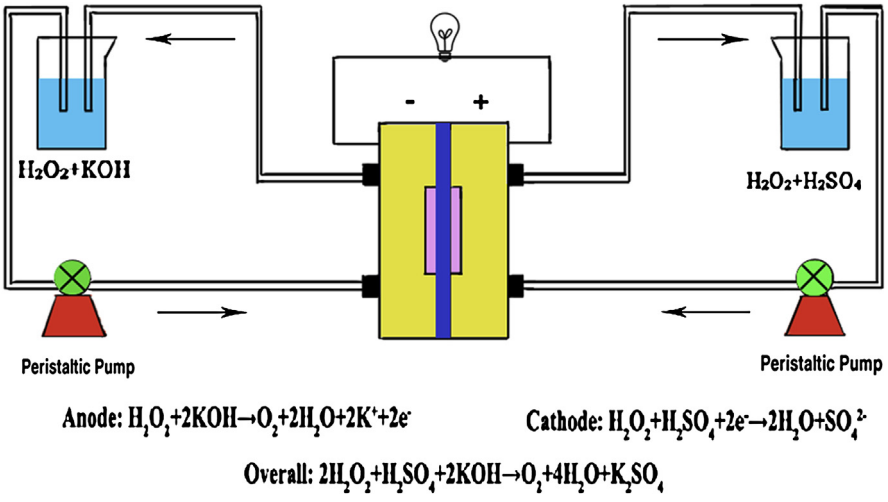

Fig. 1. A schematic representation of the direct H_2O_2–H_2O_2 fuel cell configuration.

3. Results and discussion

3.1. Characterization and electrochemical performance of the Ni/CFC and Co/CFC electrodes

Fig. 2A and B shows the SEM images of CFC substrate and Ni/CFC electrode. Carbon fiber cloth is a promising substrate owing to their unique 3D structure (Fig. 2A), good chemical stability and high electrical conductivity. The Ni catalyst was uniformly deposited on the surface of carbon fibers and covered the entire surface of CFC substrate (Fig. 2A). It has a corrugated nanostructure (Fig. 2B) making the electrode have a high surface area. Fig. 2C shows the XRD pattern of the Ni/CFC electrode. Only three sharp diffraction peaks at 44.5°, 51.8° and 76.3° were observed, which can be indexed to the diffraction from the (111), (200) and (220) planes of Ni metal according to the standard crystallographic spectrum of Ni (JCPDS card No. 65-2865), which indicated that Ni is in the metallic form rather than other Ni species, such as oxides or hydroxides. Fig. 2D shows the cyclic voltammograms (CV) of CFC and Ni/CFC electrode in 1.0 mol L^{-1} KOH at a scanning rate of 50 mV s^{-1}. The CFC substrate only showed double layer currents. The Ni/CFC electrode shows a strong oxidation peak (centered at 0.43 V) and a reduction peak (centered at 0.25 V), which is due to the redox reactions of Ni^{2+}/Ni^{3+} according to the literature [2,21].

The catalytic performance of the Ni/CFC electrode for H_2O_2 electrooxidation in alkaline solution was investigated by varying the concentration of KOH and H_2O_2, and the results were shown in Fig. 2E and F, respectively. As seen from Fig. 2E, the starting oxidation potential is ~−0.15 V and the anodic current increases with the increase of KOH concentration from 1 to 4 mol L^{-1}. Fig. 2F

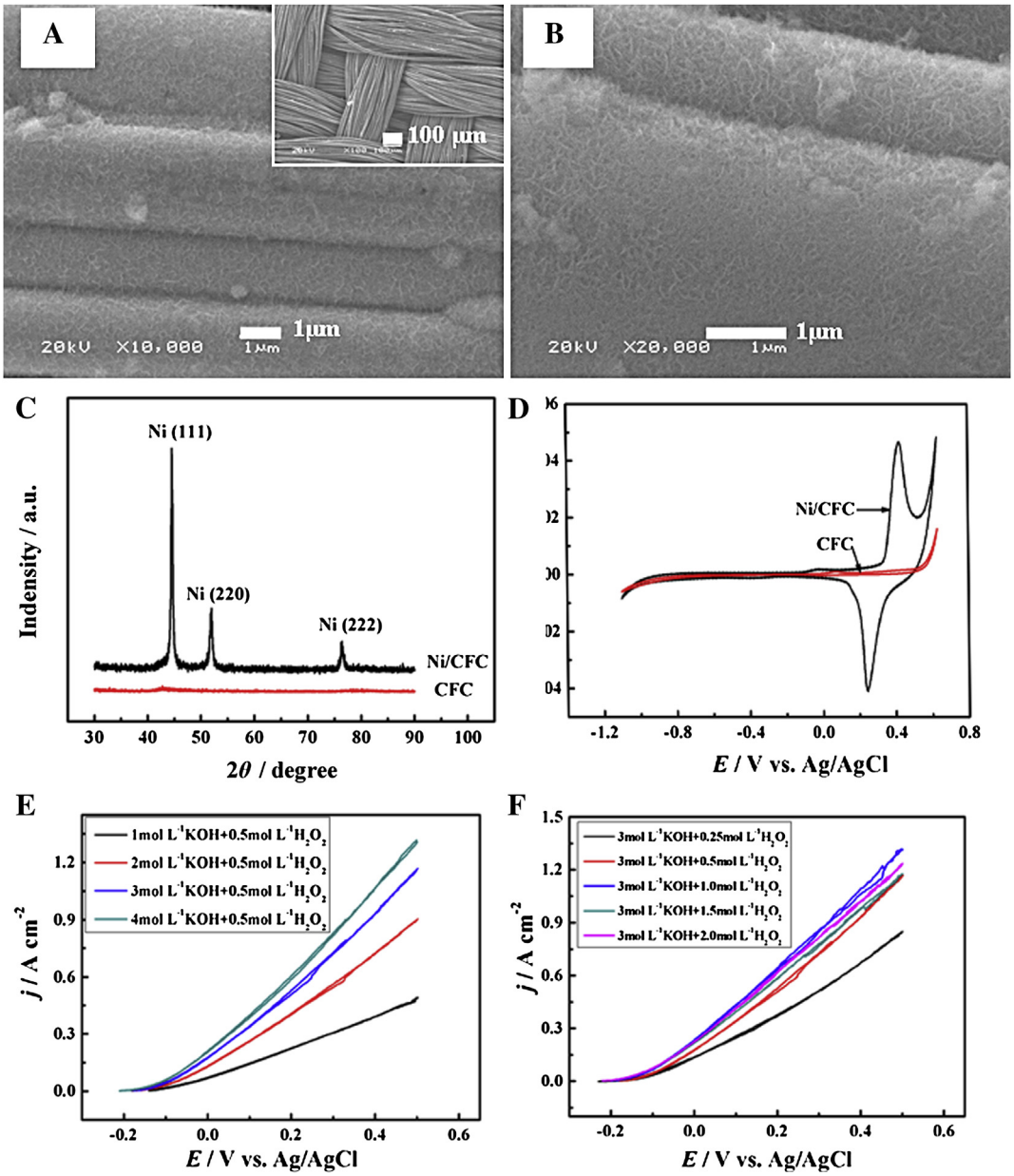

Fig. 2. Different-magnification SEM images of Ni/CFC electrode (A) and (B). XRD patterns of CFC and Ni/CFC electrode (C). Cyclic voltammograms of CFC and Ni/CFC electrode in 1.0 mol L^{-1} KOH at the scan rate of 50 mV s^{-1} (D). The effects of KOH concentration to H_2O_2 electrooxidation at Ni/CFC electrode (E). The effects of H_2O_2 concentration to H_2O_2 electrooxidation at Ni/CFC electrode (F).

demonstrated that the oxidation current was increased by increasing the H_2O_2 concentrations from 0.25 mol L^{-1} to 1.0 mol L^{-1}, but was slightly decreased with the further increase to 2.0 mol L^{-1}. Since H_2O_2 is not stable in alkaline medium, higher H_2O_2 concentration can lead to faster H_2O_2 decomposition rate.

Fig. 3A and B shows the SEM images of the Co/CFC electrode. As seen, Co film with rough surfaces was deposited on the whole surface of CFC. XRD analysis (Fig. 3C) showed that Co presents as pure metal with the peaks at 2θ = 41.7°, 44.8°,47.6° and 75.9° corresponding to the (100), (002), (101) and (110) planes of Co, respectively (JCPDS card No. 05-0727). Fig. 3D shows the CV curves of CFC and Co/CFC electrode in 1.0 mol L^{-1} KOH at a scanning rate of 50 mV s^{-1}. The CV of the Co/CFC electrode is in consistence with that of Co metal reported in the literature [22] and the redox peaks can be attributed to the inter-conversion of Co to $Co(OH)_2$ to $Co(OH)_3$.

To estimate the catalytic activity of Co/CFC electrode to H_2O_2 electrooxidation, the effects of KOH and H_2O_2 concentration were discussed in detail, which is shown in Fig. 3E and F. Fig. 3E shows the dependence of KOH concentration to H_2O_2 electrooxidation. The suitable KOH concentration should be chosen to further improve the performance of H_2O_2 electrooxidation. In Fig. 3F, H_2O_2 electrooxidation behavior is also obviously influenced by H_2O_2 concentration. Too high concentration of H_2O_2 led to no enhancement of catalytic activity. It is due to high rate of H_2O_2 decomposition producing excess O_2, which blocked surface active sites and also led to the loss of fuel.

To obtain further information on the catalytic activity of different electrocatalysts, we intended to compare the electrochemical behaviors of H_2O_2 electrooxidation on different anodes. In Table 1, we compared with the performance to H_2O_2 electrooxidation at the Ni/CFC and Co/CFC electrodes, along with Pd/CFC

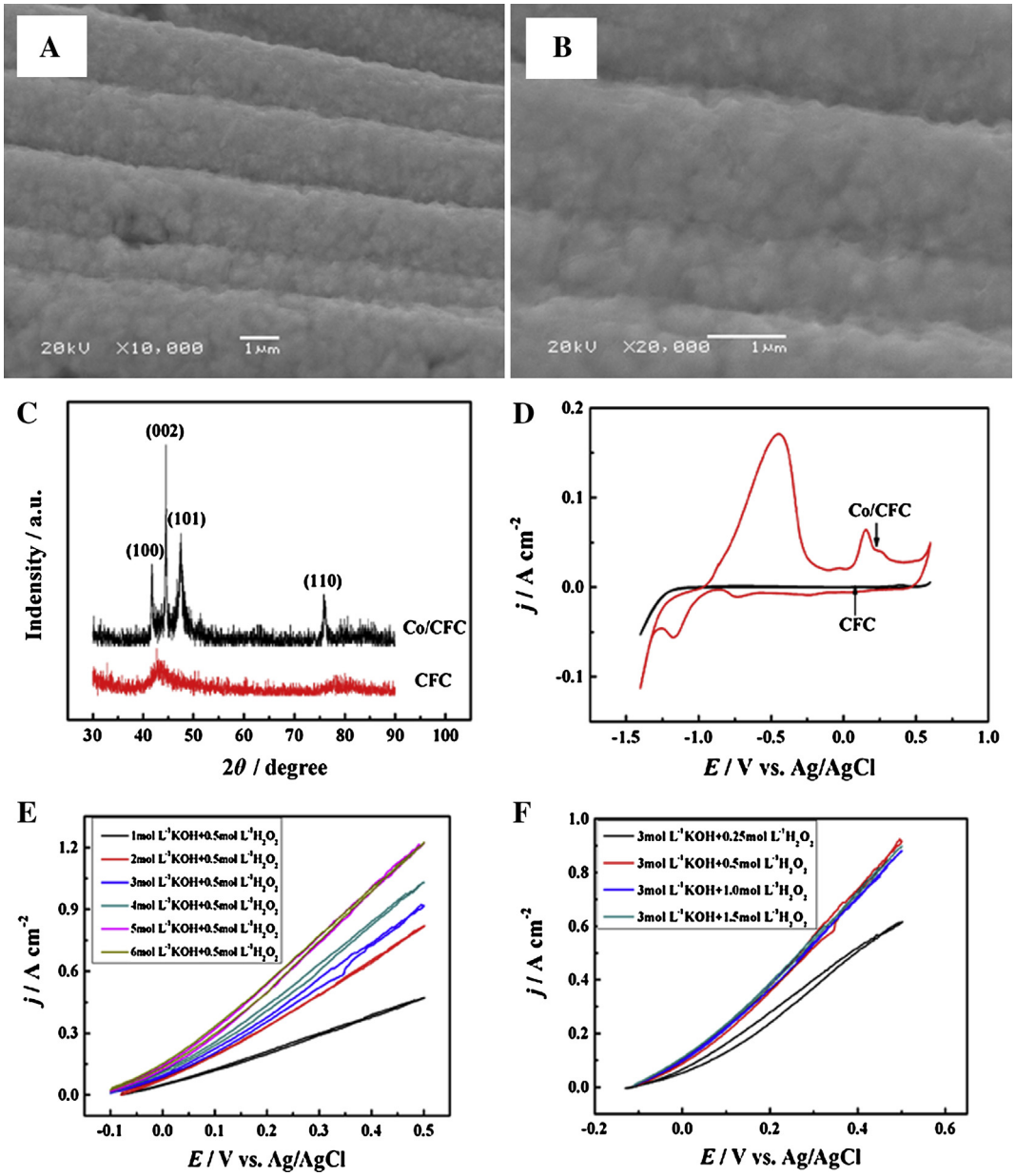

Fig. 3. Different-magnification SEM images of Co/CFC electrode (A) and (B). XRD patterns of CFC and Co/CFC electrode(C). Cyclic voltammograms of CFC and Co/CFC electrode in 1.0 mol L^{-1} KOH at the scan rate of 50 mV s^{-1} (D). The effects of KOH concentration to H_2O_2 electrooxidation at Co/CFC electrode (E). The effects of H_2O_2 concentration to H_2O_2 electrooxidation at Co/CFC electrode (F).

Table 1
The catalytic activity for H_2O_2 electrooxidation on Au/CFC, Pd/CFC, Ni/CFC and Co/CFC electrodes at 0.2 V in the solution of 3.0 mol L^{-1} KOH + 1.0 mol L^{-1} H_2O_2.

Electrode	Au/CFC	Pd/CFC	Ni/CFC	Co/CFC
Onset oxidation potential	−0.18 V	−0.18 V	−0.2 V	−0.11 V
Current density	510 mA cm^{-2}	575 mA cm^{-2}	640 mA cm^{-2}	368 mA cm^{-2}

and Au/CFC previously prepared [8,10]. Among these anodes, Ni/CFC electrode exhibited the highest catalytic activity, e.g. at 0.2 V, the oxidation current densities at Ni/CFC, Pd/CFC, Au/CFC and Co/CFC electrodes were 640 mA cm^{-2}, 575 mA cm^{-2}, 510 mA cm^{-2} and 368 mA cm^{-2}, respectively. The catalytic mechanism of Ni for H_2O_2 electrooxidation in a alkaline solution has been discussed in our recent work [23]. We believed that the reaction process involves three species including H_2O_2, OH^- and $Ni(OH)_2{\cdot}H_2O_2$ might chemically adsorbs onto $Ni(OH)_2$ to form the intermediate of $Ni(OH)_2{-}H_2O_2$, which undergoes electrochemical oxidation to form $H^+{-}Ni(OH)_2{-}H^+$ and release O_2. The $H^+{-}Ni(OH)_2{-}H^+$ reacts with OH^- to produce H_2O and regenerate $Ni(OH)_2$ species.

3.2. Performances of DPPFC with Ni/CFC and Co/CFC anodes

In order to investigate the performance of Ni/CFC and Co/CFC as the anode of DPPFC, the fuel cells with Pd/CFC cathode and Ni/CFC, Co/CFC and Au/CFC (for comparison) anode were fabricated and tested. The results are shown in Fig. 4. Clearly, the DPPFC with the Ni/CFC anode outperformed that with Au/CFC anode. However, the Au/CFC anode is better than the Co/CFC anode. The DPPFC with the Ni/CFC anode displayed an OCV of 0.9 V and a peak power density of 21.6 mW cm^{-2}, corresponding to the cell voltage of 0.6 V and a current density of 36 mA cm^{-2}. This cell performance is around 5 times higher than that reported by Sanli et al. [4] using carbon supported Ni particle as the anode catalyst, and it is also higher than that with Pd/CFC both as the anode and cathode (14.3 mW cm^{-2}) reported in our previous work [9]. Notably, the DPPFC will form a concentration cell if H_2O_2 is not added to the acid catholyte and the base anolyte. In order to examine the effect of the concentration cell on the DPPFC, the performance of the concentration cell was tested. The results showed that the concentration cell exhibited an open circuit voltage of around 0.7 V and a maximum power density is only about 0.6 mW cm^{-2} with a current density of around 1 mA cm^{-2}. This cell power density is remarkably smaller than that using H_2O_2-containing acid and base as the catholyte and anolyte, respectively. So the contribution of concentration cell can be neglected.

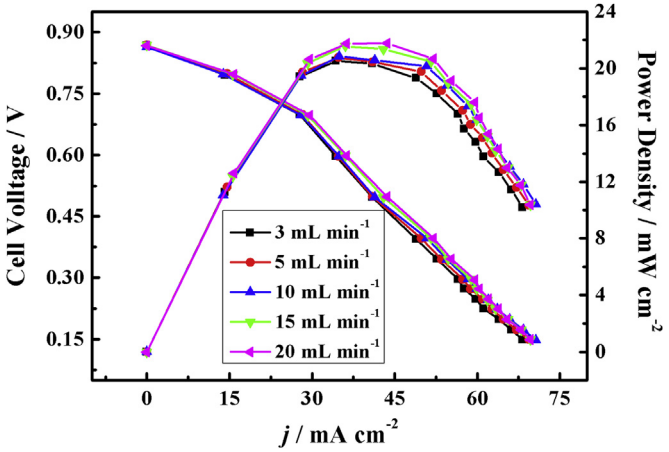

Fig. 5. Effects of the flow rate on the performance of DPPFC with Ni/CFC anode and Pd/CFC cathode. Anolyte: 4.0 mol L^{-1} KOH + 1.0 mol L^{-1} H_2O_2. Catholyte: 2.0 mol L^{-1} H_2SO_4 + 2.0 mol L^{-1} H_2O_2. Flow rate: x mL min^{-1} (x = 3, 5, 10, 15 and 20). Operation temperature: 20 °C.

Effects of flow rate and operating temperature on the performance of DPPFC with Ni/CFC anode were further investigated. The cell was operated with an anolyte of 4.0 mol L^{-1} KOH + 1.0 mol L^{-1} H_2O_2 and a catholyte of 2.0 mol L^{-1} H_2SO_4 + 2.0 mol L^{-1} H_2O_2. Fig. 5 shows the influence of flow rate on cell performance. It can be seen that the flow rate has no obvious effects on the cell performance. Fig. 6 shows the dependence of the fuel cell performance on the operation temperature. Cell performance improves remarkably by increasing the operation temperature. When the operation temperature increased from 20 to 50 °C, the peak power density increased from 21.6 to 53.8 mW cm^{-2}. It is worthy to point out that the increase of temperature will accelerate the chemical decomposition of H_2O_2, particularly in the anolyte, due to the instability of H_2O_2 in alkaline medium. The decomposition of H_2O_2 results in a decrease in the utilization efficiency of H_2O_2 fuel. The cell can deliver a maximum peak power density of 53.8 mW cm^{-2} at 109 mA cm^{-2} and 0.5 V at 50 °C, but at the expense of wasting fuel

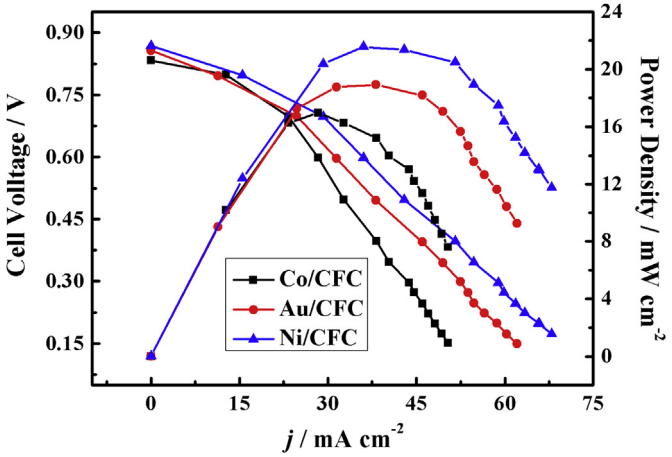

Fig. 4. The DPPFC performance with Ni/CFC, Co/CFC and Au/CFC anodes and Pd/CFC cathode. Anolyte: 4.0 mol L^{-1} KOH+1.0 mol L^{-1} H_2O_2. Catholyte: 2.0 mol L^{-1} H_2SO_4 + 2.0 mol L^{-1} H_2O_2. Flow rate: 15 mL min^{-1}. Operation temperature: 20 °C.

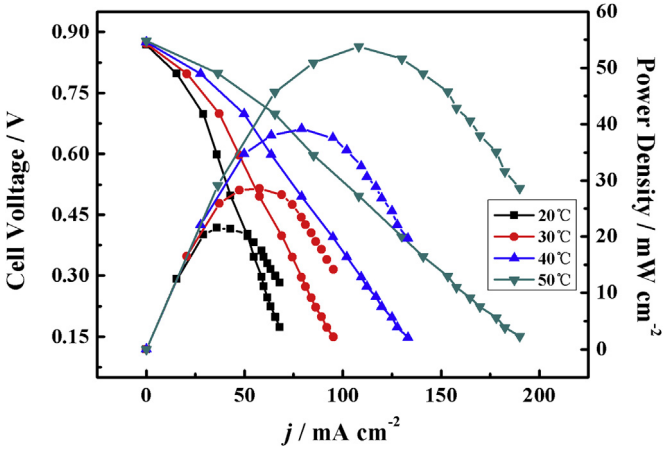

Fig. 6. Effects of operation temperature on the performance of DPPFC. Anolyte: 4.0 mol L^{-1} KOH + 1.0 mol L^{-1} H_2O_2. Catholyte: 2.0 mol L^{-1} H_2SO_4 + 2.0 mol L^{-1} H_2O_2. Flow rate: 15 mL min^{-1}.

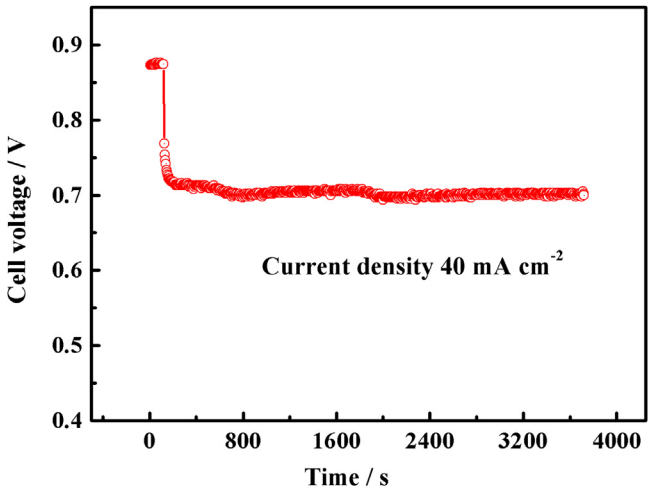

Fig. 7. Stability test of the DPPFC. Anolyte: 4.0 mol L^{-1} KOH + 1.0 mol L^{-1} H_2O_2. Catholyte: 2.0 mol L^{-1} H_2SO_4 + 2.0 mol L^{-1} H_2O_2. Flow rate: 15 mL min^{-1}. Operation temperature: 40 °C. Current density: 40 mA cm^{-2}.

and oxidant. Therefore, for a DPPFC, operating at low temperature is critical for minimizing gas evolution and achieving high utilization efficiency of the reactants.

Fig. 7 shows the curve of cell voltage *versus* time at a constant current load of 40 mA cm^{-2}. The cell was operated with an anolyte of 4.0 mol L^{-1} KOH + 1.0 mol L^{-1} H_2O_2 and a catholyte of 2.0 mol L^{-1} H_2SO_4 + 2.0 mol L^{-1} H_2O_2. The flow rate of both the anolyte and the catholyte is 15 mL min^{-1} and the temperature is 40 °C. The DPPFC was first left at the OCV for 3 min and then at 40 mA cm^{-2} for 1 h. The figure shows that the anode and cathode potentials remained constant for the duration of the experiment (>1 h) with a stable OCV of 0.9 V and a working voltage of approximately 0.7 V. During the 1 h test period, the cell voltage remained almost constant and 28 mW cm^{-2} power density was continuously generated. The excellent stability is due to the simple anode and cathode reactions involving no poisoning intermediates or products. As far as we know, such high DPPFC performance has not been previously reported.

4. Conclusions

We successfully prepared non-noble metal anodes for the application in a DPPFC, namely Ni/CFC and Co/CFC electrodes. These electrodes all exhibited high catalytic performance to H_2O_2 electrooxidation in KOH solution, even higher than noble metal catalysts (Au/CFC and Pd/CFC). The performance of DPPFCs using these anodes matched with Pd/CFC electrode (the cathode prepared in our previous work) was also systematically discussed. DPPFC with the Ni/CFC anode exhibits the highest cell performance and outperformed that with Au/CFC anode, with an OCV of 0.9 V and the peak power density of 21.6 mW cm^{-2} at 20 °C. Such high DPPFC performance has not been previously reported. The cell performance remarkably depends upon the operation temperature and is nearly independent of the flow rate of the anolyte and catholyte. The results indicated that non-precious metals can replace noble metals as the anode catalysts of DPPFC.

Acknowledgments

We gratefully acknowledge the financial support of this research by National Nature Science Foundation of China.

References

[1] F. Chen, M.-H. Chang, C.-W. Hsu, Electrochim. Acta 52 (2007) 7270–7277.
[2] S.-i. Yamazaki, Z. Siroma, H. Senoh, T. Ioroi, N. Fujiwara, K. Yasuda, J. Power Sources 178 (2008) 20–25.
[3] R.S. Disselkamp, Int. J. Hydrogen Energy 35 (2010) 1049–1053.
[4] A.E. Sanli, A. Aytaç, Int. J. Hydrogen Energy 36 (2011) 869–875.
[5] Y. Yamada, Y. Fukunishi, S.-i. Yamazaki, S. Fukuzumi, Chem. Commun. 46 (2010) 7334–7336.
[6] Y. Yamada, S. Yoshida, T. Honda, S. Fukuzumi, Energy Environ. Sci. 4 (2011) 2822–2825.
[7] S.A. Mousavi Shaegh, N.-T. Nguyen, S.M. Mousavi Ehteshami, S.H. Chan, Energy Environ. Sci. 5 (2012) 8225–8228.
[8] F. Yang, K. Cheng, Y. Mo, L. Yu, J. Yin, G. Wang, D. Cao, J. Power Sources 217 (2012) 562–568.
[9] F. Yang, K. Cheng, X. Liu, S. Chang, J. Yin, C. Du, L. Du, G. Wang, D. Cao, J. Power Sources 217 (2012) 569–573.
[10] F. Yang, K. Cheng, T. Wu, Y. Zhang, J. Yin, G. Wang, D. Cao, RSC Adv. 3 (2013) 5483–5490.
[11] K.-J. Jeong, C.M. Miesse, J.-H. Choi, J. Lee, J. Han, S.P. Yoon, S.W. Nam, T.-H. Lim, T.G. Lee, J. Power Sources 168 (2007) 119–125.
[12] E. Gyenge, Electrochim. Acta 49 (2004) 965–978.
[13] K. Yamada, K. Yasuda, H. Tanaka, Y. Miyazaki, T. Kobayashi, J. Power Sources 122 (2003) 132–137.
[14] E. Granot, B. Filanovsky, I. Presman, I. Kuras, F. Patolsky, J. Power Sources 204 (2012) 116–121.
[15] T. Lei, Y.M. Tian, G.L. Wang, J.L. Yin, Y.Y. Gao, Q. Wen, D.X. Cao, Fuel Cells 11 (2011) 431–435.
[16] G.H. Miley, N. Luo, J. Mather, R. Burton, G. Hawkins, L. Gu, E. Byrd, R. Gimlin, P.J. Shrestha, G. Benavides, J. Laystrom, D. Carroll, J. Power Sources 165 (2007) 509–516.
[17] C.P. de León, F.C. Walsh, A. Rose, J.B. Lakeman, D.J. Browning, R.W. Reeve, J. Power Sources 164 (2007) 441–448.
[18] D. Cao, Y. Gao, G. Wang, R. Miao, Y. Liu, Int. J. Hydrogen Energy 35 (2010) 807–813.
[19] W. Yang, S. Yang, W. Sun, G. Sun, Q. Xin, Electrochim. Acta 52 (2006) 9–14.
[20] S. Hasegawa, K. Shimotani, K. Kishi, H. Watanabe, Electrochem. Solid-State Lett. 8 (2005) A119–A121.
[21] X.H. Xia, J.P. Tu, Y.Q. Zhang, Y.J. Mai, X.L. Wang, C.D. Gu, X.B. Zhao, J. Phys. Chem. C 115 (2011) 22662–22668.
[22] H.-B. Noh, K.-S. Lee, P. Chandra, M.-S. Won, Y.-B. Shim, Electrochim. Acta 61 (2012) 36–43.
[23] F. Yang, K. Cheng, X. Xue, J. Yin, G. Wang, D. Cao, Electrochim. Acta (2013). in press.